

Relax-Tighten-Round Algorithm for Optimal Placement and Control of Valves and Chlorine Boosters in Water Networks

Filippo Pecci¹, Ivan Stoianov¹, Avi Ostfeld²

¹InfraSense Labs, Department of Civil and Environmental Engineering, Imperial College London, London, SW7 2BB, UK

²Faculty of Civil and Environmental Engineering Technion - Israel Institute of Technology Haifa 32000, Israel

March 2021

Abstract

In this paper, a new mixed integer nonlinear programming formulation is proposed for optimally placing and operating pressure reducing valves and chlorine booster stations in water distribution networks. The objective is the minimization of average zone pressure, while penalizing deviations from a target chlorine concentration. We propose a relax-tighten-round algorithm based on tightened polyhedral relaxations and a rounding scheme to compute feasible solutions, with bounds on their optimality gaps. This is because off-the-shelf global optimization solvers failed to compute feasible solutions for the considered non-convex mixed integer nonlinear program. The implemented algorithm is evaluated using three benchmarking water networks, and they are shown to outperform off-the-shelf solvers, for these case studies. The proposed heuristic has enabled the computation of good quality feasible solutions in most instances, with bounds on the optimality gaps that are comparable to the order of uncertainty observed in operational water network models.

1 Introduction

The main operational objectives for water utilities include the reduction of water leaks, and management of drinking-water quality. Leakage reduction is achieved by controlling average zone pressure (AZP) within water distribution networks (WDNs), while satisfying minimum service requirements [WAPS15]. Pressure control schemes are implemented through pressure reducing valves (PRVs), which reduce pressure at their downstream node. The problem of optimal placement and operation of PRVs in WDNs has been formulated in previous literature, and solved using both evolutionary algorithms [ARC06, NZ09] and mathematical optimization methods [EM12, PAS19].

Monitoring and control of disinfectant residuals in drinking water distribution networks is critical to maintain the water quality and eliminate the risks of contamination with pathogens such as bacteria and viruses in distribution [ASGK14, SLA20]. This is particularly critical during the current COVID-19 pandemic as leaking sewage from sewer networks could allow potentially harmful contaminants into drinking water networks [QWM⁺20]. In order to deactivate any pathogens that might exist in distribution networks, disinfectant is typically added at water sources (e.g. water treatment plants), with chlorine being a commonly used water disinfectant. Because chlorine

is reactive, it is depleted over time as it travels across the pipe networks, causing a reduction in the ability to prevent microbial contamination. Water utilities aim to maintain a target chlorine concentration, which is sufficient to safeguard public health, while avoiding excessive chlorination, resulting in taste and odor problems, as well as the growth of disinfection by-products. In addition, the objective is to maintain optimal and constant chlorine concentrations, as variations in chlorine concentration are perceived as water quality problems by customers. Chlorine booster stations are used to deal with this challenge [BTU⁺98, PU04]. Using booster chlorination, disinfectant is re-applied at selected locations within the network, leading to a more uniform spatial and temporal distribution of chlorine residuals. Previous literature has modeled the operation of booster stations assuming known flow velocities across network pipes - see as examples [BTU⁺98, PU04]. However, this can lead to sub-optimal design and operation of WDNs. In fact, in order to mitigate disinfectant decay reactions, network operators should aim to reduce travel time from water sources to demand nodes. This may result in sub-optimal pressure management schemes, where minimum pressure constraints are not satisfied, as observed in [KL10]. Therefore, we consider the joint optimization of hydraulic pressure and flows, together with chlorine residual concentrations in WDNs.

We investigate the problem of minimizing average zone pressure, while penalizing deviations from chlorine target concentrations, and satisfying regulatory constraints on pressure and chlorine concentration levels. [Ost05] and [KL10] implemented genetic algorithms to solve problems of optimal operation of WDNs, where optimization unknowns include network flows and chlorine concentrations, while locations of PRVs and chlorine booster stations are fixed. However, pressure reducing valves and booster stations should be optimally placed for a more effective pressure control and management of chlorine residual concentrations.

In this manuscript, we propose a new mathematical framework for the optimal placement and operation of pressure reducing valves and chlorine booster stations. The considered objective is the minimization of average zone pressure, while penalizing deviations from target chlorine concentrations at demand nodes. The transport of chlorine through each pipe is modeled by a one dimensional first-order advection PDE [RB96], where flow velocity corresponds to the one-dimensional velocity field, and a linear function is used to represent chlorine decay [HWF⁺02]. We implement an implicit upwind scheme to discretize the considered PDE. Optimization constraints include quadratic equations modelling head loss due to pipe friction [EM15, PAS17], and bilinear terms due to the presence of unknown flow velocities within the discretized advection PDE. In addition, binary variables are used to model the direction of flow across pipes, and the placement of valves and booster stations. The resulting optimization problem is a non-convex mixed integer nonlinear program.

In comparison to previous literature [Ost05, KL10], which relied on genetic algorithms, we investigate the application of mathematical optimization methods to compute feasible solutions for the considered problem, with guaranteed bounds on their optimality gaps. We propose a relax-tighen-round (RTR) algorithm based on polyhedral relaxations of the non-convex terms, an optimization-based-bound-tightening scheme, and a rounding heuristic. The developed RTR algorithm computes a feasible solution for the considered non-convex MINLP, with bounds on its optimality gap. In comparison, we show that off-the-shelf global optimization solvers failed to generate feasible solutions for the considered problem. The performance of the RTR algorithm is investigated using multiple problem instances for different WDN case studies.

2 Problem formulation

We formulate the problem of optimal placement and operation of pressure reducing valves and chlorine booster stations, with the objective of minimizing average zone pressure, while penalizing deviations from target chlorine concentrations at demand nodes. A WDN with n_n demand nodes, n_0 source nodes (e.g. water sources, water treatment plants), and n_p links is modelled as a directed graph with $n_n + n_0$ vertices and n_p edges. Define $\mathcal{P} := \{1, \dots, n_p\}$ and $\mathcal{N} := \{1, \dots, n_n\}$, $\mathcal{N}^0 := \{1, \dots, n_0\}$. Given a node $i \in \mathcal{N}$, let I_i^{in} and I_i^{out} be the index sets corresponding to links with assigned direction entering and leaving the node, respectively. We consider network operation within a discretized time interval $\mathcal{T} = 1, \dots, n_t$. The objective of this study is to minimize average zone pressure in water distribution networks, while penalizing deviation from target chlorine concentrations. Average Zone Pressure (AZP) is defined as the following weighted sum of nodal pressures [WAPS15]:

$$\sum_{k \in \mathcal{T}} \sum_{i \in \mathcal{N}} \omega_i (h_{i,k} - h_i^{\text{elev}}) \quad (1)$$

where $h_{i,k}$ is the unknown hydraulic head at node $i \in \mathcal{N}$ and time $k \in \mathcal{T}$, while $\mathbf{h}^{\text{elev}} \in \mathbb{R}^{n_n}$ is the vector of known nodal elevations. Weights are defined as follows:

$$\omega_i := \frac{\sum_{l \in I_i^{\text{in}} \cup I_i^{\text{out}}} L_l}{n_t \sum_{j \in \mathcal{N}} \sum_{l \in I_j^{\text{in}} \cup I_j^{\text{out}}} L_l}, \quad i \in \mathcal{N} \quad (2)$$

Let $\mathbf{c}^* \in \mathbb{R}^{n_n}$ be a vector of target chlorine concentration at network nodes. Moreover, set

$$\hat{d}_{i,k} = \frac{d_{i,k}}{\sum_{k \in \mathcal{T}} \sum_{j \in \mathcal{N}} d_{j,k}}, \quad i \in \mathcal{N}, k \in \mathcal{T} \quad (3)$$

where $d_{i,k}$ is the known demand at node $i \in \mathcal{N}$ and time $k \in \mathcal{T}$. Denote by $c_{i,k}$ the unknown chlorine concentration at node $i \in \mathcal{N} \cup \mathcal{N}^0$ and time $k \in \mathcal{T}$. We define the Average Target Deviation (ATD) as

$$\sum_{k \in \mathcal{T}} \sum_{i \in \mathcal{N}} \hat{d}_{i,k} |c_{i,k} - c_i^*| \quad (4)$$

The formula for ATD can be reformulated as a linear function by introducing auxiliary variables $\mu_{i,k}$, which satisfy the following linear constraints:

$$c_{i,k} - c_i^* \leq \mu_{i,k}, \quad i \in \mathcal{N}, k \in \mathcal{T} \quad (5a)$$

$$-c_{i,k} + c_i^* \leq \mu_{i,k}, \quad i \in \mathcal{N}, k \in \mathcal{T}. \quad (5b)$$

The objective function to be minimized is written as:

$$\sum_{k \in \mathcal{T}} \sum_{i \in \mathcal{N}} \omega_i h_{i,k} + \sum_{k \in \mathcal{T}} \sum_{i \in \mathcal{N}} \hat{d}_{i,k} \mu_{i,k} \quad (6)$$

Since the considered problem aims to optimize both hydraulic pressure and water quality, its formulation is based on hydraulics and water quality modelling.

2.1 Hydraulic variables and constraints

First, we introduce optimization variables and constraints related to network hydraulic properties. Source nodes are assumed to have known hydraulic heads $h_{i,k}^0$, $i \in \mathcal{N}^0$, $k \in \mathcal{T}$. We denote by $q_{l,k}$ the unknown flow in link $l \in \mathcal{P}$ at time $k \in \mathcal{T}$. The unknown frictional head loss across link l at time k is denoted by $\theta_{l,k}$. Pressure control valves reduce pressure at their downstream node, introducing additional head losses, which are represented by variable $\eta_{l,k}$, $l \in \mathcal{P}$, $k \in \mathcal{T}$. Vector of binary variables $\mathbf{v} \in \{0,1\}^{2n_p}$ models the placement of control valves. We have:

$$v_l = \begin{cases} 1 & \text{a valve is placed on link } l \text{ in the positive flow direction} \\ 0 & \text{otherwise,} \end{cases} \quad (7)$$

and

$$v_{n_p+l} = \begin{cases} 1 & \text{a valve is placed on link } l \text{ in the negative flow direction} \\ 0 & \text{otherwise.} \end{cases} \quad (8)$$

These binary variables are subject to the following physical and economical constraints:

$$v_l + v_{n_p+l} \leq 1, \quad l \in \mathcal{P} \quad (9a)$$

$$\sum_{l \in \mathcal{P}} (v_l + v_{n_p+l}) = n_v \quad (9b)$$

The following constraints formulate energy and mass conservation laws, and the placement of pressure reducing valves on network links:

$$h_{i_1,k} - h_{i_2,k} = \theta_{l,k} + \eta_{l,k}, \quad i_1 \xrightarrow{l} i_2, l \in \mathcal{P}, i_1 \in \mathcal{N}, i_2 \in \mathcal{N}, k \in \mathcal{T} \quad (10a)$$

$$h_{i_1,k}^0 - h_{i_2,k} = \theta_{l,k} + \eta_{l,k}, \quad i_1 \xrightarrow{l} i_2, l \in \mathcal{P}, i_1 \in \mathcal{N}^0, i_2 \in \mathcal{N}, k \in \mathcal{T} \quad (10b)$$

$$\sum_{l \in I_i^{\text{in}}} q_{l,k} - \sum_{l \in I_i^{\text{out}}} q_{l,k} = d_{i,k}, \quad i \in \mathcal{N}, k \in \mathcal{T} \quad (10c)$$

$$\eta_{l,k} - \eta_{l,k}^{\max} v_l \leq 0, \quad l \in \mathcal{P}, k \in \mathcal{T} \quad (10d)$$

$$-\eta_{l,k} + \eta_{l,k}^{\min} v_{n_p+l} \leq 0, \quad l \in \mathcal{P}, k \in \mathcal{T} \quad (10e)$$

$$-q_{l,k} - q_{l,k}^{\min} v_l \leq -q_{l,k}^{\min}, \quad l \in \mathcal{P}, k \in \mathcal{T} \quad (10f)$$

$$q_{l,k} + q_{l,k}^{\max} v_{n_p+l} \leq q_{l,k}^{\max}, \quad l \in \mathcal{P}, k \in \mathcal{T} \quad (10g)$$

In order to model the transport of chlorine constituent, it is required to explicitly consider the flow direction across network links as a decision variable. Therefore, we introduce auxiliary variables $q_{l,k}^+$, $q_{l,k}^-$, $\theta_{l,k}^+$, $\theta_{l,k}^-$, $s_{l,k}$, and binary variable $z_{l,k} \in \{0,1\}$ such that

$$q_{l,k} = q_{l,k}^+ - q_{l,k}^-, \quad l \in \mathcal{P}, k \in \mathcal{T} \quad (11a)$$

$$s_{l,k} = q_{l,k}^+ + q_{l,k}^-, \quad l \in \mathcal{P}, k \in \mathcal{T} \quad (11b)$$

$$\theta_{l,k} = \theta_{l,k}^+ - \theta_{l,k}^-, \quad l \in \mathcal{P}, k \in \mathcal{T} \quad (11c)$$

$$0 \leq q_{l,k}^+ \leq (q^+)_{l,k}^{\max} z_{l,k}, \quad l \in \mathcal{P}, k \in \mathcal{T} \quad (11d)$$

$$0 \leq q_{l,k}^- \leq (q^-)_{l,k}^{\max} (1 - z_{l,k}), \quad l \in \mathcal{P}, k \in \mathcal{T} \quad (11e)$$

$$0 \leq \theta_{l,k}^+ \leq (\theta^+)_{l,k}^{\max} z_{l,k}, \quad l \in \mathcal{P}, k \in \mathcal{T} \quad (11f)$$

$$0 \leq \theta_{l,k}^- \leq (\theta^-)_{l,k}^{\max} (1 - z_{l,k}), \quad l \in \mathcal{P}, k \in \mathcal{T} \quad (11g)$$

Frictional head losses are often represented by either the Hazen-Williams (H-W) or the Darcy-Weisbach (D-W) equations [DLWB15]. Since both formulae involve non-smooth terms, quadratic approximations have been proposed and used in previous literature [EM15, PAS17]. Let $\mathbf{a} \in \mathbb{R}^{n_p}$ and $\mathbf{b} \in \mathbb{R}^{n_p}$ be vector of coefficients of these approximations. We enforce the following constraints on variables $\theta_{l,k}^+$ and $\theta_{l,k}^-$:

$$\theta_{l,k}^+ = a_l(q_{l,k}^+)^2 + b_l q_{l,k}^+, \quad l \in \mathcal{P}, k \in \mathcal{T} \quad (12a)$$

$$\theta_{l,k}^- = a_l(q_{l,k}^-)^2 + b_l q_{l,k}^-, \quad l \in \mathcal{P}, k \in \mathcal{T}. \quad (12b)$$

Constraints $z_{l,k} \in \{0, 1\}$, (11), and (12) are equivalent to the non-linear equations:

$$s_{l,k} = |q_{l,k}|, \quad l \in \mathcal{P}, k \in \mathcal{T} \quad (13a)$$

$$q_{l,k}^+ = \max(q_{l,k}, 0), \quad l \in \mathcal{P}, k \in \mathcal{T} \quad (13b)$$

$$q_{l,k}^- = -\min(q_{l,k}, 0), \quad l \in \mathcal{P}, k \in \mathcal{T} \quad (13c)$$

$$\theta_{l,k}^+ = \max(\theta_{l,k}, 0), \quad l \in \mathcal{P}, k \in \mathcal{T} \quad (13d)$$

$$\theta_{l,k}^- = -\min(\theta_{l,k}, 0), \quad l \in \mathcal{P}, k \in \mathcal{T}, \quad (13e)$$

$$z_{l,k} = \frac{1 + \text{sign}(q_{l,k})}{2}, \quad l \in \mathcal{P}, k \in \mathcal{T}, \quad (13f)$$

and

$$\theta_{l,k} = a_l |q_{l,k}| q_{l,k} + b_l q_{l,k}, \quad l \in \mathcal{P}, k \in \mathcal{T}, \quad (14)$$

where $\text{sign}(q_{l,k}) = 1$ if $q_{l,k} > 0$, and $\text{sign}(q_{l,k}) = -1$ otherwise. Lower and upper bounds on hydraulic variables are given by

$$q_{l,k}^{\min} \leq q_{l,k} \leq q_{l,k}^{\max}, \quad l \in \mathcal{P}, k \in \mathcal{T} \quad (15a)$$

$$h_{i,k}^{\min} \leq h_{i,k} \leq h_{i,k}^{\max}, \quad i \in \mathcal{N}, k \in \mathcal{T} \quad (15b)$$

$$\eta_{l,k}^{\min} \leq \eta_{l,k} \leq \eta_{l,k}^{\max}, \quad l \in \mathcal{P}, k \in \mathcal{T} \quad (15c)$$

$$\theta_{l,k}^{\min} \leq \theta_{l,k} \leq \theta_{l,k}^{\max}, \quad l \in \mathcal{P}, k \in \mathcal{T} \quad (15d)$$

and

$$(q^+)_{l,k}^{\min} \leq q_{l,k}^+ \leq (q^+)_{l,k}^{\max}, \quad l \in \mathcal{P}, k \in \mathcal{T} \quad (16a)$$

$$(q^-)_{l,k}^{\min} \leq q_{l,k}^- \leq (q^-)_{l,k}^{\max}, \quad l \in \mathcal{P}, k \in \mathcal{T} \quad (16b)$$

$$(\theta^+)_{l,k}^{\min} \leq \theta_{l,k}^+ \leq (\theta^+)_{l,k}^{\max}, \quad l \in \mathcal{P}, k \in \mathcal{T} \quad (16c)$$

$$(\theta^-)_{l,k}^{\min} \leq \theta_{l,k}^- \leq (\theta^-)_{l,k}^{\max}, \quad l \in \mathcal{P}, k \in \mathcal{T} \quad (16d)$$

$$s_{l,k}^{\min} \leq s_{l,k} \leq s_{l,k}^{\max}, \quad l \in \mathcal{P}, k \in \mathcal{T}. \quad (16e)$$

2.2 Water quality variables and constraints

Next, we describe variables and constraints associated with water quality. Let $c_{i,k}^{\max}$ be the maximum allowed chlorine concentration at network node $i \in \mathcal{N} \cup \mathcal{N}^0$ and time $k \in \mathcal{T}$. The evolution of chlorine concentration along a given link $l \in \mathcal{P}$ is governed by a PDE modelling advective

transport of constituent with first order decay [RB96]. We implement an Eulerian implicit upwind discretization scheme, where backward differences are used to approximate both temporal and spatial derivatives [ICC99]. For each link $l \in \mathcal{P}$, we introduce a space discretization $j\Delta x_l$, $j \in \{0, \dots, J_l\}$, with $\Delta x_l = \frac{L_l}{J_l}$, where L_l is the length of link l . We denote by $r_{j,l,k}$ the chlorine concentration at $j\Delta x_l$ and time k , for all $j \in \{0, \dots, J_l\}$ and $k \in \{0, \dots, n_t\}$. We also have auxiliary variables $w_{j,l,k}$ such that:

$$w_{j,l,k} = s_{l,k} r_{j,l,k}, \quad j = 0, \dots, J_l, \quad l \in \mathcal{P}, \quad k \in \mathcal{T}, \quad (17)$$

For all $j \in \{1, \dots, J_l\}$, $l \in \mathcal{P}$, and $k \in \mathcal{T}$, the discretized PDE yields:

$$(1 + \alpha_l \Delta t) r_{j,l,k} - r_{j,l,k-1} + \gamma_l (w_{j,l,k} - w_{j-1,l,k}) = 0, \quad (18)$$

where $\gamma_l = (4\Delta t)/(10^3 \pi D_l^2 \Delta x_l)$, with L_l and D_l length and diameter of link l , respectively, and $\alpha_l > 0$ is the first order decay coefficient associated with pipe l [HWF⁺02]. Initial concentrations in pipes are defined as

$$r_{j,l,0} = c_{i_2}^0, \quad \forall j \in \{0, \dots, J_l\}, \quad \forall l \in \mathcal{P}, \quad i_1 \xrightarrow{l} i_2 \quad (19)$$

with given initial concentration c_i^0 at node $i \in \mathcal{N} \cup \mathcal{N}^0$. Furthermore, $r_{0,l,k}$ is assumed to be equal to the concentration of the upstream node, depending on the flow direction:

$$r_{0,l,k} - c_{i_1,k} + c_{i_2}^{\max} z_{l,k} \leq c_{i_2}^{\max} \quad (20a)$$

$$-r_{0,l,k} + c_{i_1,k} + c_{i_1}^{\max} z_{l,k} \leq c_{i_1}^{\max} \quad (20b)$$

$$r_{0,l,k} - c_{i_2,k} - c_{i_1}^{\max} z_{l,k} \leq 0 \quad (20c)$$

$$-r_{0,l,k} + c_{i_2,k} - c_{i_2}^{\max} z_{l,k} \leq 0, \quad (20d)$$

Our problem formulation considers as free decision variables concentrations at source nodes $c_{i,k}$, $i \in \mathcal{N}^0$. Moreover, let $\mathbf{v}^b \in \{0, 1\}^{n_b}$ be a vector of binary decision variables, modelling the placement of a chlorine booster station at network nodes, i.e. $v_i^b = 1$ if a chlorine booster station is placed at node i , $v_i^b = 0$, otherwise. The number of boosters considered for installation is enforced by the linear constraint:

$$\mathbf{1}^T \mathbf{v}^b = n_b \quad (21)$$

Chlorine concentration at unknown head node $i \in \mathcal{N}$ and time $k \in \mathcal{T}$ is governed by the following mixing equations:

$$c_{i,k} d_{i,k} + \sum_{l \in I_i^{\text{in}}} (w_{0,l,k} - \rho_{l,k}) + \sum_{l \in I_i^{\text{out}}} (\rho_{l,k} - w_{N_l,l,k}) - \xi_{i,k} = 0 \quad (22a)$$

$$0 \leq \xi_{i,k} \leq \xi_{i,k}^{\max} v_i^b, \quad (22b)$$

where slack variable $\xi_{i,k} \geq 0$ is introduced to model the additional constituent mass injected by a booster, and $\xi_{i,k}^{\max}$ are sufficiently large positive constants, for all $i \in \mathcal{N}$, and $k \in \mathcal{T}$. In addition, auxiliary variables $\rho_{l,k}$ are subject to the following linear constraints:

$$0 \leq \rho_{l,k} \leq \rho_{l,k}^{\max} z_{l,k} \quad (23a)$$

$$w_{0,l,k} + w_{N_l,l,k} - \rho_{l,k} - \rho_{l,k}^{\max} z_{l,k} \leq \rho_{l,k}^{\max} \quad (23b)$$

$$-w_{0,l,k} - w_{N_l,l,k} + \rho_{l,k} \leq 0 \quad (23c)$$

Finally, we include the following lower and upper bounds:

$$0 \leq c_{i,k} \leq c_i^{\max}, \quad i \in \mathcal{N} \cup \mathcal{N}^0, k \in \mathcal{T}, \quad (24a)$$

$$0 \leq r_{j,l,k} \leq r_{j,l}^{\max}, \quad j = 0, \dots, J_l, l \in \mathcal{P}, k \in \mathcal{T}, \quad (24b)$$

$$0 \leq w_{j,l,k} \leq w_{j,l,k}^{\max}, \quad j = 0, \dots, J_l, l \in \mathcal{P}, k \in \mathcal{T}, \quad (24c)$$

$$0 \leq \rho_{l,k} \leq \rho_{l,k}^{\max}, \quad l \in \mathcal{P}, k \in \mathcal{T}, \quad (24d)$$

$$0 \leq \xi_{i,k} \leq \xi_{i,k}^{\max}, \quad i \in \mathcal{N}, k \in \mathcal{T}. \quad (24e)$$

2.3 Mixed Integer Non-linear Program

The problem of optimal placement and control of valves and chlorine boosters aims to minimize (6), subject to non-convex quadratic constraints (12) and (17), and linear constraints (5), (9), (10), (11), (15), (16), (18), (20), (21), (22), (23), (24). The optimization problem considers both continuous and binary variables. We write the problem in compact form, defining vectors $\mathbf{x} := [\mathbf{q} \ \mathbf{h} \ \boldsymbol{\eta} \ \boldsymbol{\theta}]^T$, $\mathbf{u} := [\mathbf{s} \ \mathbf{q}^+ \ \mathbf{q}^- \ \boldsymbol{\theta}^+ \ \boldsymbol{\theta}^-]^T$, and $\mathbf{y} := [\mathbf{c} \ \mathbf{r} \ \mathbf{w} \ \boldsymbol{\rho} \ \boldsymbol{\xi} \ \boldsymbol{\mu}]^T$. Consider the following Mixed Integer Non-linear Program (MINLP):

$$\min_{\substack{\mathbf{x}, \mathbf{u}, \mathbf{z} \\ \mathbf{y}, \mathbf{v}, \mathbf{v}^b}} f_{\text{AZP}}(\mathbf{x}) + f_{\text{ATD}}(\mathbf{y}) \quad (25a)$$

$$\text{s.t.} \quad \mathbf{F}\mathbf{u} = \text{diag}(\mathbf{A}\mathbf{u})\mathbf{A}\mathbf{u} + \mathbf{B}\mathbf{u} \quad (25b)$$

$$\mathbf{W}\mathbf{y} = \text{diag}(\mathbf{S}\mathbf{u})\mathbf{R}\mathbf{y} \quad (25c)$$

$$\mathbf{M}\mathbf{x} + \mathbf{N}\mathbf{u} + \mathbf{P}\mathbf{z} \leq \mathbf{p} \quad (25d)$$

$$\mathbf{x} \in X(\mathbf{v}), \mathbf{v} \in V \quad (25e)$$

$$\mathbf{y} \in Y(\mathbf{z}, \mathbf{v}^b) \quad (25f)$$

$$\mathbf{1}^T \mathbf{v}^b = n_b \quad (25g)$$

$$\mathbf{z} \in \{0, 1\}^{n_t n_p}, \mathbf{v} \in \{0, 1\}^{2n_p}, \mathbf{v}^b \in \{0, 1\}^{n_n}, \quad (25h)$$

where, given a vector $\mathbf{e} \in \mathbb{R}^N$, $\text{diag}(\mathbf{e}) \in \mathbb{R}^{N \times N}$ is the diagonal matrix with diagonal entries equal to the components of vector \mathbf{e} . Linear functions $f_{\text{AZP}}(\cdot)$ and $f_{\text{ATD}}(\cdot)$ are such that (25a) corresponds to (6). Matrices \mathbf{F} , \mathbf{A} , and \mathbf{B} are defined so that the rows of (25b) correspond to the non-convex quadratic constraints (12). Matrices \mathbf{W} , \mathbf{S} , and \mathbf{R} are opportunely defined so that the rows of (25c) correspond to (17). The set V is defined by linear constraints (9). Given $\mathbf{v} \in V$, we denote by $X(\mathbf{v})$ the polyhedral set defined by constraints (10) and (15). Moreover, \mathbf{M} , \mathbf{N} , \mathbf{P} , and \mathbf{p} are defined so that the rows of (25d) correspond to constraints (11) and (16). Finally, given vectors \mathbf{v}^b and \mathbf{z} , we define $Y(\mathbf{v}^b, \mathbf{z})$ as the polyhedral set defined by constraints (5), (18), (20), (22), (23), (24). Problem (25) has $n_t(8n_p + 4n_n + 2\bar{J} + n_0)$ continuous variables, $n_t n_p + 2n_p + n_n$ binary variables, and $n_t(2n_p + \bar{J})$ non-convex quadratic constraints, where $\bar{J} = \sum_{l \in \mathcal{P}} (1 + J_l)$. Therefore, even for small water networks, it results in large non-convex MINLPs, which are difficult to solve - see Table 1.

3 Solution algorithm

The considered MINLP (25) combines difficulties in handling non-convex constraints with the presence of integer decision variables. In addition, the formulation of Problem (25) includes a

discretized PDE for each network link, resulting in a large number of continuous variables and non-convex constraints, even for small size WDNs - see Table 1.

We investigate the performance of off-the-shelf solvers to compute solutions for Problem (25), considering two case study network models, namely `2loopsNet` and `pescara` - see Section 4 for network properties and layouts. We formulate Problem (25) in `2loopsNet` for $n_v \in \{1, 2, 3\}$ and $n_b = n_v$, and `pescara` for $n_v \in \{1, 2, 3, 4, 5\}$ and $n_b = n_v$ - a total of 8 experiments. This study considers the global optimization solvers `BARON` [TS02], `scip` [GEG⁺17], `LINDOGlobal` [Lin20], and `Couenne` [BLL⁺09]. Moreover, we investigate the ability of solvers `Bonmin` [BBC⁺08], `Knitro` [Art20], `Ipopt` [WB06], and `AlphaECP` [WP02] to compute feasible solutions to Problem (25). We refer to these as local solvers, because they do not provide guarantees of global optimality when considering non-convex MINLPs like Problem (25). All experiments are performed on NEOS Server for Optimization [CMM98], with a time limit of 6 hours. Since `Ipopt` does not directly handle problems with binary constraints, we have substituted them with the following complementary constraints:

$$\begin{aligned} \text{diag}(\mathbf{z})(\mathbf{1} - \mathbf{z}) &= \mathbf{0} \\ \text{diag}(\mathbf{v})(\mathbf{1} - \mathbf{v}) &= \mathbf{0} \\ \text{diag}(\mathbf{v}^b)(\mathbf{1} - \mathbf{v}^b) &= \mathbf{0} \end{aligned} \tag{26}$$

The results of these experiments are summarized in Tables A1 - A16 of Appendix 2. When considering the small case study `2loopsNet`, `BARON` and `SCIP` were able to compute feasible solutions for $n_v \in \{2, 3\}$. Moreover, local solvers `AlphaECP` and `Bonmin` have computed feasible solutions only when $n_v = 2$. In comparison, `LINDOGlobal`, `Couenne`, `Knitro` and `Ipopt` failed to compute feasible solutions for all problem instances considering `2loopsNet`. Furthermore, none of the tested solvers was able to compute feasible solutions for problem instances considering `pescara`. As off-the-shelf solvers were not able to compute feasible solutions in most tested instances, we propose an algorithm to compute feasible solutions for Problem (25), together with bounds on their optimality gaps.

We propose the relax-tighten-round (RTR) algorithm, which combines a rounding heuristic with the solution of a continuous polyhedral relaxation of the non-convex MINLP in Problem (25), tightened using an optimization-based bound-tightening (OBBT) scheme. If successful, the algorithm computes a lower bound LB and an upper bound UB to the optimal value of Problem (25). A worst-case estimate on optimality gap of the computed solution is given by:

$$\text{Gap} := 100 \frac{\text{UB} - \text{LB}}{\text{LB}} \tag{27}$$

In order to evaluate the obtained bounds on the optimality gaps, it is important to take into account the range of uncertainties that are inherent in hydraulic and water quality modelling of water networks. For example, [WAPS15] and [WPS20] showed that uncertainties affecting pressure control of operational water networks can result in up to 20% relative difference between simulated and measured pressure at network nodes. We expect the uncertainty range to be of the same magnitude and possibly higher for chlorine residuals.

The steps necessary to derive the RTR algorithm are detailed in the following sub-sections. Section 3.1 presents a rounding heuristic to compute feasible solutions of Problem (25). In Section 3.2, we introduce polyhedral relaxations of the non-convex constraints in Problem (25). Then, Section 3.3 describes the OBBT procedure to tighten the relaxation, and Section 3.4 presents the overall RTR algorithm.

3.1 Rounding heuristic

Firstly, we describe a heuristic to compute a feasible solution of Problem (25), given a vector of fractional values $\mathbf{v} \in [0, 1]^{2n_p} \cap V$. Let $J_{n_v} \subset \{1, \dots, 2n_p\}$ be the set of indices corresponding to the n_v largest elements in \mathbf{v} , where only the largest value between v_l and v_{n_p+l} is considered for each link $l = 1, \dots, n_p$. For all $l = 1, \dots, 2n_p$, define:

$$\hat{v}_l = \begin{cases} 1 & \text{if } l \in J_{n_v} \\ 0 & \text{otherwise.} \end{cases} \quad (28)$$

This rounding scheme yields a vector $\hat{\mathbf{v}} \in V \cap \{0, 1\}^{2n_p}$. Next, we obtain a feasible solution of Problem (25). Observe that only constraints (25c) and (25f) couple vectors of hydraulic variables $\mathbf{x}, \mathbf{u}, \mathbf{z}$ with water quality vectors \mathbf{y}, \mathbf{v}^b . We implement a two-stage approach, where hydraulic and water quality quantities are optimized in sequence. We consider the following MINLP:

$$\min_{\mathbf{x}, \mathbf{u}, \mathbf{z}} f_{\text{AZP}}(\mathbf{x}) \quad (29a)$$

$$\text{s.t. } \mathbf{F}\mathbf{u} = \text{diag}(\mathbf{A}\mathbf{u})\mathbf{A}\mathbf{u} + \mathbf{B}\mathbf{u} \quad (29b)$$

$$\mathbf{M}\mathbf{x} + \mathbf{N}\mathbf{u} + \mathbf{P}\mathbf{z} \leq \mathbf{p} \quad (29c)$$

$$\mathbf{x} \in X(\hat{\mathbf{v}}), \mathbf{z} \in \{0, 1\}^{n_t n_p}. \quad (29d)$$

Problem (29) includes $n_t n_p$ integer variables, and it is difficult to solve even for small/medium water networks. We have observed that $\mathbf{z} \in \{0, 1\}^{n_t n_p}$, (11), and (12) are equivalent to non-linear equations (13) and (14). Since (29b) and (29c) correspond to constraints (12) and (11), respectively, Problem (29) is equivalent to the following non-linear program:

$$\min_{\mathbf{x}} f_{\text{AZP}}(\mathbf{x}) \quad (30a)$$

$$\text{s.t. } \mathbf{g}(\mathbf{x}) = \mathbf{0} \quad (30b)$$

$$\mathbf{x} \in X(\hat{\mathbf{v}}) \quad (30c)$$

where $\mathbf{g}(\cdot)$ is a non-linear function such that $\mathbf{g}(\mathbf{x})$ is the vector whose components are the rows of equalities (14). Let $\hat{\mathbf{x}} = [\hat{\mathbf{q}} \ \hat{\mathbf{h}} \ \hat{\boldsymbol{\eta}} \ \hat{\boldsymbol{\theta}}]^T$ be a locally optimal solution of Problem (30) computed by a NLP solver. We recover a feasible solution of Problem (29) by defining vectors $\hat{\mathbf{u}} = [\hat{\mathbf{s}} \ \hat{\mathbf{q}}^+ \ \hat{\mathbf{q}}^- \ \hat{\boldsymbol{\theta}}^+ \ \hat{\boldsymbol{\theta}}^-]^T$ and $\hat{\mathbf{z}}$ using (13). Finally, let $(\hat{\mathbf{y}}, \hat{\mathbf{v}}^b)$ be solution of the mixed integer linear program (MILP):

$$\min_{\mathbf{y}, \mathbf{v}^b} f_{\text{ATD}}(\mathbf{y})$$

$$\text{s.t. } \mathbf{W}\mathbf{y} = \text{diag}(\mathbf{S}\hat{\mathbf{u}})\mathbf{R}\mathbf{y}$$

$$\mathbf{y} \in Y(\hat{\mathbf{z}}, \mathbf{v}^b) \quad (31)$$

$$\mathbf{1}^T \mathbf{v}^b = n_b$$

$$\mathbf{v}^b \in \{0, 1\}^{n_b}.$$

Since constraints in Problems (29) and (31) correspond to constraints in Problem (25), we conclude that $(\hat{\mathbf{x}}, \hat{\mathbf{u}}, \hat{\mathbf{z}}, \hat{\mathbf{y}}, \hat{\mathbf{v}}, \hat{\mathbf{v}}^b)$ is a feasible solution for Problem (25).

3.2 Polyhedral relaxation

In order to compute a lower bound to the optimal value of Problem (25), we formulate a convex relaxation of the considered non-convex MINLP. Note that the non-convex terms in (25b) and (25c) are the only non-linear terms within the formulation of Problem (25). To take advantage of numerically efficient algorithms for solving linear programs, it is convenient to consider linear relaxations of these non-convex terms. First, we consider polyhedral relaxations of matrix equation (25b). Since each row in (25b) corresponds to a quadratic equation in (12), a polyhedral relaxation of (25b) is obtained by relaxing each row individually. As shown in Appendix 1, this results in the following linear equations:

$$\mathbf{F}\mathbf{u} \geq \text{diag}(\mathbf{A}\mathbf{u}^{(i)})\mathbf{A}(2\mathbf{u} - \mathbf{u}^{(i)}) + \mathbf{B}\mathbf{u}, \quad i = 1, \dots, m \quad (32a)$$

$$\mathbf{F}\mathbf{u} \leq \text{diag}(\mathbf{A}\mathbf{u}^{\min} + \mathbf{A}\mathbf{u}^{\max})\mathbf{A}\mathbf{u} + \mathbf{B}\mathbf{u} - \text{diag}(\mathbf{A}\mathbf{u}^{\min})\mathbf{A}\mathbf{u}^{\max} \quad (32b)$$

for given vectors $\mathbf{u}^{\min} = \mathbf{u}^{(1)} < \mathbf{u}^{(1)} < \dots < \mathbf{u}^{(m)} = \mathbf{u}^{\max}$, where equality and inequality operators are to be interpreted element-wise. The polyhedral relaxations (32) have the advantage of resulting in linear programs, which can be efficiently solved by state-of-the art linear programming solvers.

The bilinear terms (17) are relaxed via the Reformulation Linearization Technique (RLT) [SA99]. These relaxations are given by:

$$\mathbf{W}\mathbf{y} \geq \text{diag}(\mathbf{S}\mathbf{u}^{\min})\mathbf{R}\mathbf{y} + \text{diag}(\mathbf{R}\mathbf{y}^{\min})\mathbf{S}\mathbf{u} - \text{diag}(\mathbf{S}\mathbf{u}^{\min})\mathbf{S}\mathbf{y}^{\min} \quad (33a)$$

$$\mathbf{W}\mathbf{y} \geq \text{diag}(\mathbf{S}\mathbf{u}^{\max})\mathbf{R}\mathbf{y} + \text{diag}(\mathbf{R}\mathbf{y}^{\max})\mathbf{S}\mathbf{u} - \text{diag}(\mathbf{S}\mathbf{u}^{\max})\mathbf{S}\mathbf{y}^{\max} \quad (33b)$$

$$\mathbf{W}\mathbf{y} \leq \text{diag}(\mathbf{S}\mathbf{u}^{\max})\mathbf{R}\mathbf{y} + \text{diag}(\mathbf{R}\mathbf{y}^{\min})\mathbf{S}\mathbf{u} - \text{diag}(\mathbf{S}\mathbf{u}^{\max})\mathbf{S}\mathbf{y}^{\min} \quad (33c)$$

$$\mathbf{W}\mathbf{y} \leq \text{diag}(\mathbf{S}\mathbf{u}^{\min})\mathbf{R}\mathbf{y} + \text{diag}(\mathbf{R}\mathbf{y}^{\max})\mathbf{S}\mathbf{u} - \text{diag}(\mathbf{S}\mathbf{u}^{\min})\mathbf{S}\mathbf{y}^{\max} \quad (33d)$$

where inequalities are to be interpreted element-wise. Finally, observe that Problem (25) includes a large number of binary variables, which results in impractical computational effort even for medium size water networks - see Table 1. Therefore, we consider the following continuous polyhedral relaxation of Problem (25), where we also relax the binary constraints:

$$\begin{aligned} & \min_{\substack{\mathbf{x}, \mathbf{u}, \mathbf{z} \\ \mathbf{y}, \mathbf{v}, \mathbf{v}^b}} f_{\text{AZP}}(\mathbf{x}) + f_{\text{ATD}}(\mathbf{y}) \\ \text{s.t.} \quad & \mathbf{F}\mathbf{u} \geq \text{diag}(\mathbf{A}\mathbf{u}^{(i)})\mathbf{A}(2\mathbf{u} - \mathbf{u}^{(i)}) + \mathbf{B}\mathbf{u}, \quad i = 1, \dots, m \\ & \mathbf{F}\mathbf{u} \leq \text{diag}(\mathbf{A}\mathbf{u}^{\min} + \mathbf{A}\mathbf{u}^{\max})\mathbf{A}\mathbf{u} + \mathbf{B}\mathbf{u} - \text{diag}(\mathbf{A}\mathbf{u}^{\min})\mathbf{A}\mathbf{u}^{\max} \\ & \mathbf{W}\mathbf{y} \geq \text{diag}(\mathbf{S}\mathbf{u}^{\min})\mathbf{R}\mathbf{y} + \text{diag}(\mathbf{R}\mathbf{y}^{\min})\mathbf{S}\mathbf{u} - \text{diag}(\mathbf{S}\mathbf{u}^{\min})\mathbf{S}\mathbf{y}^{\min} \\ & \mathbf{W}\mathbf{y} \geq \text{diag}(\mathbf{S}\mathbf{u}^{\max})\mathbf{R}\mathbf{y} + \text{diag}(\mathbf{R}\mathbf{y}^{\max})\mathbf{S}\mathbf{u} - \text{diag}(\mathbf{S}\mathbf{u}^{\max})\mathbf{S}\mathbf{y}^{\max} \\ & \mathbf{W}\mathbf{y} \leq \text{diag}(\mathbf{S}\mathbf{u}^{\max})\mathbf{R}\mathbf{y} + \text{diag}(\mathbf{R}\mathbf{y}^{\min})\mathbf{S}\mathbf{u} - \text{diag}(\mathbf{S}\mathbf{u}^{\max})\mathbf{S}\mathbf{y}^{\min} \\ & \mathbf{W}\mathbf{y} \leq \text{diag}(\mathbf{S}\mathbf{u}^{\min})\mathbf{R}\mathbf{y} + \text{diag}(\mathbf{R}\mathbf{y}^{\max})\mathbf{S}\mathbf{u} - \text{diag}(\mathbf{S}\mathbf{u}^{\min})\mathbf{S}\mathbf{y}^{\max} \\ & \mathbf{M}\mathbf{x} + \mathbf{N}\mathbf{u} + \mathbf{P}\mathbf{z} \leq \mathbf{p} \\ & \mathbf{x} \in X(\mathbf{v}), \mathbf{v} \in V \\ & \mathbf{y} \in Y(\mathbf{z}, \mathbf{v}^b) \\ & \mathbf{1}^T \mathbf{v}^b = n_b \\ & \mathbf{z} \in [0, 1]^{n_t n_p}, \mathbf{v} \in [0, 1]^{2n_p}, \mathbf{v}^b \in [0, 1]^{n_n}. \end{aligned} \quad (34)$$

3.3 Optimization-Based Bound-Tightening

The tightness of relaxations (32) and (33), depends on vectors \mathbf{u}^{\min} and \mathbf{u}^{\max} , whose elements are lower and upper bounds on hydraulic auxiliary variables (16). Equations (13) and (14) imply that elements of \mathbf{u}^{\min} and \mathbf{u}^{\max} are functions of lower and upper bounds on the flow variables $q_{l,k}$, $l \in \mathcal{P}$, $k \in \mathcal{T}$. Hence, we consider an optimization-based bound-tightening (OBBT) scheme, to reduce the domain of the flow variables. We expect flow variables to be primarily influenced by hydraulic variables and constraints in Problem (25). Hence, for all $\sigma \in \{-1, 1\}$, $l \in \mathcal{P}$, and $k \in \mathcal{T}$, we consider:

$$\begin{aligned}
& \min_{\mathbf{x}, \mathbf{u}, \mathbf{z}, \mathbf{v}} \sigma \mathbf{e}_{(l,k)}^T \mathbf{x} \\
& \text{s.t.} \quad \mathbf{F}\mathbf{u} \geq \text{diag}(\mathbf{A}\mathbf{u}^{(i)})\mathbf{A}(2\mathbf{u} - \mathbf{u}^{(i)}) + \mathbf{B}\mathbf{u}, \quad i = 1, \dots, m \\
& \quad \mathbf{F}\mathbf{u} \leq \text{diag}(\mathbf{A}(\mathbf{u}^{\min} + \mathbf{u}^{\max}))\mathbf{A}\mathbf{u} + \mathbf{B}\mathbf{u} - \text{diag}(\mathbf{A}\mathbf{u}^{\min})\mathbf{A}\mathbf{u}^{\max} \\
& \quad \mathbf{M}\mathbf{x} + \mathbf{N}\mathbf{u} + \mathbf{P}\mathbf{z} \leq \mathbf{p} \\
& \quad \mathbf{x} \in X(\mathbf{v}), \mathbf{v} \in V \\
& \quad \mathbf{z} \in [0, 1]^{n_t n_p}, \mathbf{v} \in [0, 1]^{2n_p}.
\end{aligned} \tag{35}$$

where $\mathbf{e}_{(l,k)}$ is an opportunely defined vector, which selects variable $q_{l,k}$ from vector \mathbf{x} . However, solving $2n_t n_p$ Problems (35) would require a significant computational effort even for small/medium size water networks. We investigate an alternative approach, aimed at solving smaller linear programs than (35). Observe that matrices \mathbf{F} , \mathbf{A} , \mathbf{B} , \mathbf{M} , \mathbf{N} , and \mathbf{P} are block diagonal with respect to the time index $k \in \mathcal{T}$, as they correspond to constraints (11) and (12). Let \mathbf{F}_k , \mathbf{A}_k , \mathbf{B}_k , \mathbf{M}_k , \mathbf{N}_k and \mathbf{P}_k be the diagonal blocks, respectively, for all $k \in \mathcal{T}$. In addition, let \mathbf{x}_k , \mathbf{u}_k , \mathbf{z}_k be the sub-vectors of \mathbf{x} , \mathbf{u} , \mathbf{z} whose components correspond to time index $k \in \mathcal{T}$. We denote by $X_k(\mathbf{v})$ the polyhedral set defined by constraints (10) considering only time index $k \in \mathcal{T}$. Finally, we introduce new vectors of variables $\tilde{\mathbf{v}}_k \in \mathbb{R}^{2n_p}$, $k \in \mathcal{T}$. The following problem is equivalent to Problem (35):

$$\begin{aligned}
& \min_{\substack{\mathbf{x}, \mathbf{u}, \mathbf{z} \\ \mathbf{v}, \tilde{\mathbf{v}}}} \sigma \mathbf{e}_{(l,k)}^T \mathbf{x} \\
& \text{s.t.} \quad \mathbf{F}_k \mathbf{u}_k \geq \text{diag}(\mathbf{A}_k \mathbf{u}_k^{(i)}) \mathbf{A}_k (2\mathbf{u}_k - \mathbf{u}_k^{(i)}) + \mathbf{B}_k \mathbf{u}_k, \quad i = 1, \dots, m, \quad k \in \mathcal{T} \\
& \quad \mathbf{F}_k \mathbf{u}_k \leq \text{diag}(\mathbf{A}_k (\mathbf{u}_k^{\min} + \mathbf{u}_k^{\max})) \mathbf{A}_k \mathbf{u}_k + \mathbf{B}_k \mathbf{u}_k - \text{diag}(\mathbf{A}_k \mathbf{u}_k^{\min}) \mathbf{A}_k \mathbf{u}_k^{\max}, \quad k \in \mathcal{T} \\
& \quad \mathbf{M}_k \mathbf{x}_k + \mathbf{N}_k \mathbf{u}_k + \mathbf{P}_k \mathbf{z}_k \leq \mathbf{p}_k, \quad k \in \mathcal{T} \\
& \quad \mathbf{x}_k \in X_k(\tilde{\mathbf{v}}_k), \tilde{\mathbf{v}}_k \in V, \quad k \in \mathcal{T} \\
& \quad \mathbf{z}_k \in [0, 1]^{n_p}, \tilde{\mathbf{v}}_k \in [0, 1]^{2n_p}, \quad k \in \mathcal{T} \\
& \quad \tilde{\mathbf{v}}_k = \mathbf{v}, \quad k \in \mathcal{T}.
\end{aligned} \tag{36}$$

Removing the time-coupling constraints on vectors \mathbf{v} and $\tilde{\mathbf{v}}$, Problem (36) becomes separable with respect to $k \in \mathcal{T}$. The considered OBBT scheme solves $2n_t n_p$ linear programs of the form:

$$\begin{aligned}
& \min_{\mathbf{x}_k, \mathbf{u}_k, \mathbf{z}_k, \tilde{\mathbf{v}}_k} \quad \sigma \mathbf{e}_{(l)}^T \mathbf{x}_k \\
& \text{s.t.} \quad \mathbf{F}_k \mathbf{u}_k \geq \text{diag}(\mathbf{A}_k \mathbf{u}_k^{(i)}) \mathbf{A}_k (2\mathbf{u}_k - \mathbf{u}_k^{(i)}) + \mathbf{B}_k \mathbf{u}_k, \quad i = 1, \dots, m \\
& \quad \mathbf{F}_k \mathbf{u}_k \leq \text{diag}(\mathbf{A}_k (\mathbf{u}_k^{\min} + \mathbf{u}_k^{\max})) \mathbf{A}_k \mathbf{u}_k + \mathbf{B}_k \mathbf{u}_k - \text{diag}(\mathbf{A}_k \mathbf{u}_k^{\min}) \mathbf{A} \mathbf{u}_k^{\max} \quad (37) \\
& \quad \mathbf{M}_k \mathbf{x}_k + \mathbf{N}_k \mathbf{u}_k + \mathbf{P}_k \mathbf{z}_k \leq \mathbf{p}_k \\
& \quad \mathbf{x}_k \in X_k(\tilde{\mathbf{v}}_k), \tilde{\mathbf{v}}_k \in V \\
& \quad \mathbf{z}_k \in [0, 1]^{n_p}, \tilde{\mathbf{v}}_k \in [0, 1]^{2n_p}.
\end{aligned}$$

where $\mathbf{e}_{(l)}$ is a vector used to select element $q_{l,k}$ from vector \mathbf{x}_k , for all $\sigma \in \{-1, 1\}$, $k \in \mathcal{T}$, and $l \in \mathcal{P}$. The OBBT scheme is summarized in Algorithm 1.

Algorithm 1 Optimization-based bound-tightening (OBBT)

Output: tightened vectors \mathbf{u}^{\min} and \mathbf{u}^{\max} .
for $l \in \mathcal{P}$ **do**
 for $k \in \mathcal{T}$ **do**
 Tighten $q_{l,k}^{\min}$ by solving Problem (37) with $\sigma = 1$.
 Tighten $q_{l,k}^{\max}$ by solving Problem (37) with $\sigma = -1$.
 Update \mathbf{u}^{\min} and \mathbf{u}^{\max} using (13) and (14).
 end for
end for

3.4 Algorithm implementation

The RTR algorithm is summarized in Algorithm 2. At each iteration $i \in \{1, \dots, I^{\max}\}$, we solve Problem (34), computing the optimal value $\text{LB}(i)$, and a corresponding vector $\mathbf{v}^{(i)} \in V \cap [0, 1]^{2n_p}$. Since Problem (34) is a polyhedral relaxation of the original non-convex Problem (25), we have that $\text{LB}(i)$ is a lower bound to the optimal value of Problem (25). Next, we implement the rounding scheme to obtain a vector $\hat{\mathbf{v}}^{(i)} \in V \cap \{0, 1\}^{2n_p}$, and apply a NLP solver to compute a locally optimal solution to Problem (30) with $\hat{\mathbf{v}} = \hat{\mathbf{v}}^{(i)}$. If the NLP solver is successful, we store the computed locally optimal solution. If the termination criterion is not satisfied, we implement Algorithm 1 and proceed with a new iteration. The iterative procedure stops either when the maximum number of iterations has been reached, or the relative change in lower bounds computed in consecutive iterations is smaller than the tolerance. Then, we select the locally optimal solution of Problem (30) resulting in the smallest value of $f_{\text{AZP}}(\cdot)$, and refer to the corresponding vectors as \mathbf{x}^* , \mathbf{u}^* , \mathbf{z}^* , \mathbf{v}^* . We also select the largest lower bound value LB . Finally, we compute \mathbf{y}^* , $(\mathbf{v}^b)^*$ by solving the MILP (31) with $\hat{\mathbf{u}} = \mathbf{u}^*$ and $\hat{\mathbf{z}} = \mathbf{z}^*$. When successful, the RTR algorithm terminates with a feasible solution for Problem (25), given by \mathbf{x}^* , \mathbf{u}^* , \mathbf{z}^* , \mathbf{v}^* , \mathbf{y}^* , $(\mathbf{v}^b)^*$. As consequence, we also obtain an upper bound to the optimal value of Problem (25), given by $\text{UB} = f_{\text{AZP}}(\mathbf{x}^*) + f_{\text{ATD}}(\mathbf{y}^*)$. Observe that the NLP solver does not need to compute the globally optimal solution to the non-convex Problem (30), as it is sufficient to compute a feasible solution to generate an upper bound for Problem (25).

Algorithm 2 Relax-Tighten-Round (RTR)

- 1: Initialize ϵ_{tol} , I_{max} , and set $i = 1$.
- 2: **for** $i = 1, \dots, I_{\text{max}}$ **do**
- 3: Solve Problem (34) computing $\text{LB}(i)$ (the optimal value) and $\mathbf{v}^{(i)}$.
- 4: Implement rounding scheme (28) and obtain $\hat{\mathbf{v}}^{(i)}$.
- 5: Compute a locally optimal solution to Problem (30) with $\hat{\mathbf{v}} = \hat{\mathbf{v}}^{(i)}$.
- 6: If successful, let $f_{\text{AZP}}^{(i)}$ be the corresponding objective function value.
- 7: **if** $i \leq I_{\text{max}} - 1$ **and** ($i = 1$ **or** $\frac{|\text{LB}(i) - \text{LB}(i-1)|}{\text{LB}(i-1)} > \epsilon_{\text{tol}}$) **then**
- 8: Implement Algorithm 1 to tighten \mathbf{u}^{\min} and \mathbf{u}^{\max} .
- 9: **else**
- 10: Terminate loop.
- 11: **end if**
- 12: **end for**
- 13: Set $f_{\text{AZP}}^* = \min_i f_{\text{AZP}}^{(i)}$ and $\text{LB} = \max_i \text{LB}(i)$.
- 14: Let \mathbf{x}^* and \mathbf{v}^* be the vectors corresponding to the best locally optimal solution found, and define \mathbf{u}^* and \mathbf{z}^* using (13).
- 15: Solve Problem (31) with $\hat{\mathbf{z}} = \mathbf{z}^*$, $\hat{\mathbf{u}} = \mathbf{u}^*$, obtaining \mathbf{y}^* and $(\mathbf{v}^b)^*$.
- 16: Set $\text{UB} = f_{\text{AZP}}(\mathbf{x}^*) + f_{\text{ATD}}(\mathbf{y}^*)$

4 Case studies and results

We evaluate the RTR algorithm on different benchmark water distribution network models, with varying size and level of connectivity. All LPs and MILPs are solved using the state-of-the-art solver **GUROBI** (v9.0) [Gur20], while the nonlinear programs are solved using the solver for large-scale optimization **Ipopt** (v3.12.9) [WB06]. In the implementation of **Ipopt**, we supply gradients and Jacobians to the solver, in order to take advantage of the sparse structure of optimization problems in water networks.

We consider a published benchmark network, referred to as **21loopsNet** [Ost05]. In addition, we formulate and solve the problem of optimal valve and chlorine booster placement using **pescara** and **modena**, originally presented by [BDL⁺12]. In order to obtain more realistic problem instances, we have introduced temporal and spatial variability of demand profiles and Hazen-Williams roughness coefficients, respectively. We have also added first-order chlorine decay coefficients to network pipes. All case study models consider 24 hours of network operation, with a time step of one hour (i.e. $n_t = 24$). Network hydraulic models and bounds on hydraulic heads and pipe flows are provided at <http://dx.doi.org/10.17632/ws9pwxkbb2.3>. The layout of **21loopsNet** is presented in Figure 1a. The network has $n_n = 6$ demand nodes, $n_p = 10$ links, and $n_0 = 3$ water inlets. Case study **pescara** include $n_n = 68$ nodes and $n_p = 99$ links, and $n_0 = 3$ water inlets - see Figure 1b. Finally, for **modena** we have $n_n = 268$, $n_p = 317$, and $n_0 = 4$ - see Figure 1c. Note that the considered case study networks result in large non-convex MINLPs, with a significant number of binary variables and non-convex terms - see Table 1.

In order to initialize nodal chlorine concentrations, we simulate 24 hours of network operation using the software for hydraulic and water quality analysis **EPANET** [RB96], with fixed chlorine concentrations at inlets equal to 0.5 mg/l. We define c^0 in equation (18) as the nodal concentrations at 24:00 hours computed by the **EPANET** simulation. In the formulation of Problem (25), maximum

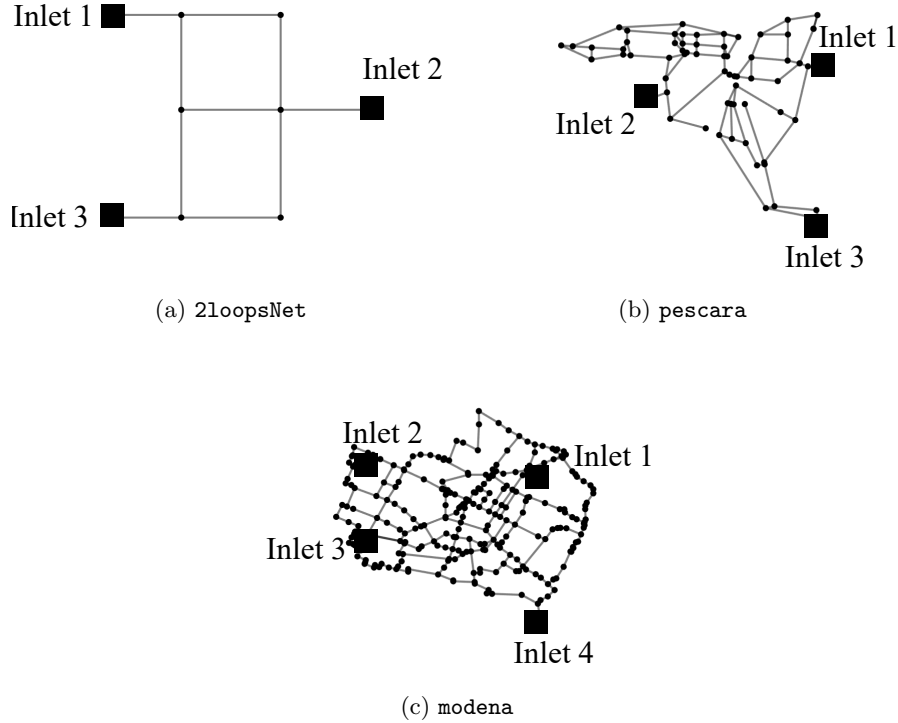


Figure 1: Case study network layouts.

Table 1: Problem size for the 3 case study networks.

	# Cont. var.	# Bin. var.	# Non-convex cons.
2loopsNet	4008	266	1200
pescara	39432	2615	11760
modena	132336	8510	38040

allowed concentration at demand nodes is set 2 mg/l, while chlorine concentrations at network inlets are not allowed to be greater than 0.5 mg/l. The target concentration at demand nodes is 1 mg/l. Finally, in (18), we set a temporal time step $\Delta t = 3600s$ (1 hour) and $\Delta x_l = \frac{L_l}{2}$, where L_l is the length of link l , for all $l = 1, \dots, n_p$. We set $m = 5$ in (32) as preliminary experiments have shown that this setting results in sufficiently tight polyhedral relaxations, for all case studies. In addition, we have observed that the lower bounds computed by the RTR algorithm do not significantly improve after the first few iterations. Hence, we set $\epsilon_{\text{tol}} = 10^{-2}$ and $I_{\text{max}} = 10$ in Algorithm 2. Our choice is also supported by the results summarized in Table 2, which shows that the number of iterations performed by Algorithm 2 is never larger than 5.

We formulate Problem (25) for $n_v \in \{1, 2, 3\}$ and $n_b \in \{0, \dots, 3\}$ in **2loopsNet**, and $n_v \in \{1, \dots, 5\}$ and $n_b \in \{0, \dots, 5\}$ in **pescara** and **modena**. Hence, we consider a total of 72 different formulations of Problem (25), and we implement the RTR Algorithm 2 to compute feasible solutions with bounds on their optimality gaps - see Appendix 2 in the supplementary material for tables of results. In contrast to the off-the-shelf solvers considered in Section 3, RTR has computed feasible

solutions in all problem instances for **2loopsNet** and **pescara**. In the case of **modena**, RTR has not returned a feasible solution only when $n_v = 5$. As reported in Appendix 2, the computed relative optimality gaps in problem instances for **2loopsNet** and **modena** are never larger than 20%. In comparison, in the case of **pescara**, the relative optimality gaps are between 25% and 35%. Optimality gaps of such magnitude are comparable to the order of uncertainty affecting hydraulic models of operational water networks [WAPS15, WPS20]. Hence, the RTR algorithm results in good quality solutions for the vast majority of problem instances.

Table 2 reports the computational effort required by RTR to compute feasible solutions for the tested problem instances. We set N_{AZP} equal to the number of iterations required by **Ipopt** when computing a locally optimal solution for Problem (30). Moreover, we denote by N_{RTR} the number of iterations of RTR Algorithm 2. The number of calls of the OBBT Algorithm 1 is then $N_{RTR} - 1$, while the number of **Ipopt** calls within Algorithm 2 is equal to N_{RTR} . Table 2 shows that **Ipopt** is able to compute locally optimal solutions to Problem (30) within 30 iterations for most problem instances. Moreover, these results show that the computational time required by RTR algorithm for **2loops** and **pescara** is significantly smaller than six hours (21600 s), the time limit set for the off-the-shelf solvers considered in Section 3. We also compare the lower bounds obtained by

Table 2: (a) Minimum, (b) mean, and (c) maximum number of iterations and CPU time for the considered solvers and algorithms. N_{AZP} =number of iterations of IPOPT when applied to Problem (30), N_{RTR} =number of iterations in RTR algorithm.

	2loops			pescara			modena		
	(a)	(b)	(c)	(a)	(b)	(c)	(a)	(b)	(c)
N_{RTR}	3	3	3	3	4	5	2	3	4
N_{AZP}	12	12	12	15	21	23	15	28	100
Time (s)	5	6	7	210	677	1387	1045	3027	10132

RTR with those computed by the off-the-shelf global optimization solvers **BARON**, **scip**, **Couenne**, and **LINDOGlobal** - see Tables A1-A8 in Appendix 2. Recall that we implemented these solvers for solving instances of Problem (25) formulated for $n_v \in \{1, 2, 3\}$ in **2looppNet**, and $n_v \in \{1, 2, 3, 4, 5\}$ in **pescara**. Let LB^{OTS} be the largest lower bound computed by the off-the-shelf solvers, for each experiment. We denote with LB^{RTR} the lower bound computed by RTR for the same problem instances. As reported in Table 3, the off-the-shelf global optimization solvers computed slightly better lower bounds in the case of **2looppNet**, with the largest difference roughly equal to 3.4%. In comparison, in the case of **pescara**, the lower bounds computed by RTR are up to 18% tighter than the best lower bounds obtained by the off-the-shelf solvers. We conclude that RTR has enabled the computation of lower bounds that are comparable to those obtained by off-the-shelf global optimization solvers after six hours of computations on the NEOS server.

In Figure 2, we report the computed AZP values for the feasible solutions obtained by RTR. For the same number of installed valves n_v , the computed AZP values for $n_b = 0, \dots, 5$ are the same. As it should be expected, feasible solutions computed for increasing number of valves correspond to decreasing values of AZP.

Analogously, the average target deviation for nodal concentrations is reduced as additional chlorine booster stations are installed - see Figure 3. Without any chlorine booster station, there is limited ability to control chlorine concentrations, using only the injected concentrations at water sources, which, in our formulation, can not be greater than 0.5 (mg/l). As we install more booster stations, the system is able to maintain nodal concentrations closer to the target.

Table 3: Comparison between lower bounds computed by RTR and off-the-shelf-solvers.

2loopsNet				pescara			
n_v	n_b	LB ^{RTR}	LB ^{OTS}	n_v	n_b	LB ^{RTR}	LB ^{OTS}
1	1	99.63	102.05	1	1	34.60	28.30
2	2	95.66	98.37	2	2	26.44	23.75
3	3	93.13	96.43	3	3	22.28	21.82
				4	4	21.04	21.45
				5	5	20.32	21.01

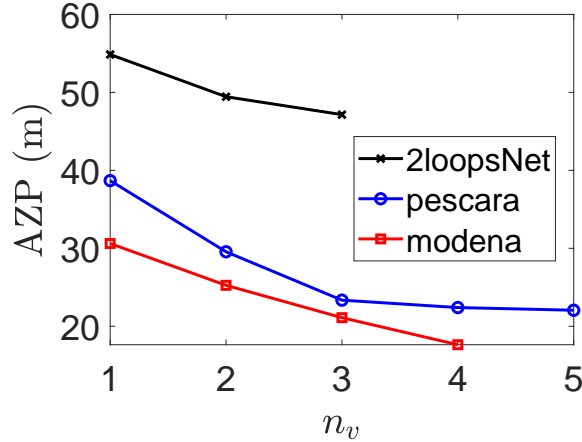


Figure 2: AZP values for the considered problem instances.

Observe that the best possible value of ATD is 0. However, several hours are required for nodal concentrations to reach the optimized level, following the installation and operation of chlorine booster stations. If the travel time between a newly installed booster station and a specific node is T^{age} hours, we expect nodal concentrations to reflect the action of the booster station after T^{age} hours. In addition, network topology and spatial distribution of decay coefficients can affect the ability to control chlorine concentrations at selected locations. Therefore, we do not expect nodal concentrations to be exactly equal to the target at all time steps.

5 Conclusions

We have proposed a new mixed integer nonlinear programming formulation for the problem of optimal placement and operation of pressure reducing valves and chlorine booster stations in water distribution networks. The numerical experiments reported in this manuscript show that off-the-shelf global optimization solvers can fail to compute feasible solutions for the considered problem, and the computed lower bounds to the optimal value are not tight. We have implemented polyhedral relaxations and a bound-tightening scheme resulting in improved lower bounds compared to off-the-shelf solvers. Furthermore, we have proposed the Relax-Tighten-Round (RTR) algorithm as heuristic to compute feasible solutions for the considered problem. The developed RTR algorithm has been evaluated by solving multiple problem instances for three case study networks. RTR is

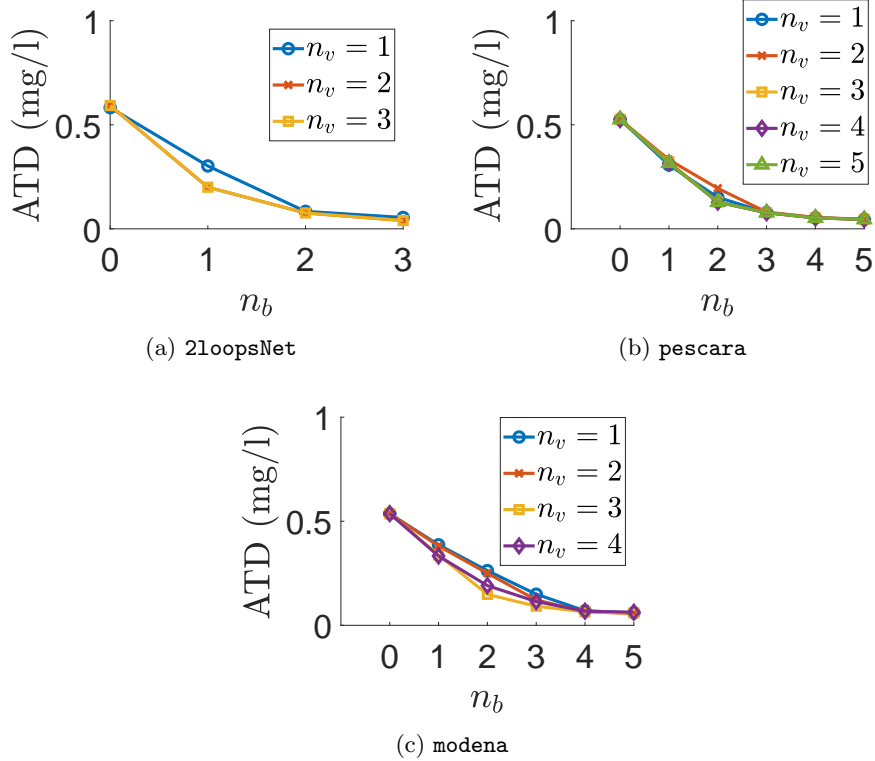


Figure 3: optimized ATD values for the three case study networks.

shown to outperform off-the-shelf solvers for the considered case studies. In addition, the developed heuristic has enabled the computation of good quality feasible solutions for the vast majority of the considered problem instances, with bounds on the optimality gaps that are comparable to the order of uncertainty affecting hydraulic models of operational water networks.

The proposed problem formulation and RTR algorithm enable the joint optimization of pressure and disinfectant dosage in water distribution networks. This allows water utilities to implement integrated and efficient schemes for pressure and water quality management, in order to minimize leakage and protect public health. Future work should extend the problem formulation to include the operation of pumps and water tanks within the same optimization framework. Moreover, the proposed polyhedral relaxations could be tightened, for example implementing semidefinite or second-order cone relaxations of the non-convex quadratic constraints.

Appendix 1: polyhedral relaxation of quadratic head loss equation

We consider the non-convex quadratic constraint:

$$\theta = aq^2 + bq \quad (\text{A38})$$

with $q \in [q^{\min}, q^{\max}]$, $q^{\min} \geq 0$. A convex relaxation of (A38), is given by:

$$\begin{aligned} \theta &\geq aq^2 + bq \\ \theta &\leq a(q^{\min} + q^{\max})q + bq - aq^{\min}q^{\max} \end{aligned} \quad (\text{A39})$$

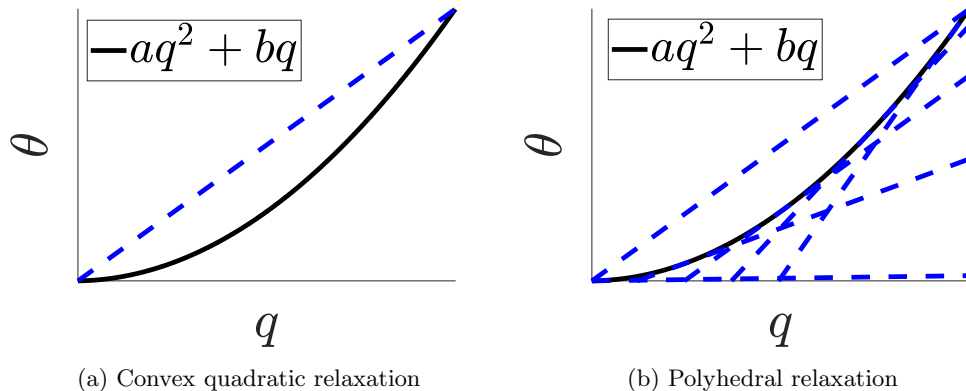


Figure A4: Convex relaxations of the head loss equation.

This is illustrated in Figure A4a, where inequalities in (A39) define the area between the curve and the dashed line. We can also further relax (A39), considering a linear outer approximation of the convex quadratic inequality constraint:

$$\begin{aligned}
 \theta &\geq a(q^{(i)})^2 + 2aq^{(i)}(q - q^{(i)}) + bq, \quad i = 1, \dots, m \\
 \theta &\leq a(q^{\min} + q^{\max})q + bq - aq^{\min}q^{\max}
 \end{aligned}
 \tag{A40}$$

where $q^{\min} = q^{(1)} < \dots < q^{(m)} = q^{\max}$ are equidistant points with $m \geq 2$. Equation (A40) defines a polyhedral relaxation of (A38) - Figure A4b shows an example with $m = 5$. Finally, observe that (A40) can equivalently re-written as:

$$\begin{aligned}
 \theta &\geq a(q^{(i)})(2q - q^{(i)}) + bq, \quad i = 1, \dots, m \\
 \theta &\leq a(q^{\min} + q^{\max})q + bq - aq^{\min}q^{\max}
 \end{aligned}
 \tag{A41}$$

Appendix 2: tables of results

Table A4: Results obtained by BARON for 2loopsNet.

n_v	n_b	UB	LB	CPU Time (s)	Status
1	1	—	100.79	21600	No solution
2	2	100.75	97.28	21600	Integer solution
3	3	97.92	92.12	21600	Integer solution

Table A5: Results obtained by BARON for pescara.

n_v	n_b	UB	LB	CPU Time (s)	Status
1	1	—	22.56	21600	No solution
2	2	—	21.32	21600	No solution
3	3	—	20.65	21600	No solution
4	4	—	21.34	21600	No solution
5	5	—	21.01	21600	No solution

Table A6: Results obtained by scip for 2loopsNet.

n_v	n_b	UB	LB	CPU Time (s)	Status
1	1	—	102.05	21600	No solution
2	2	100.72	98.37	21600	Integer solution
3	3	97.88	96.43	21600	Integer solution

Table A7: Results obtained by scip for pescara.

n_v	n_b	UB	LB	CPU Time (s)	Status
1	1	—	28.3	21600	No solution
2	2	—	23.76	21600	No solution
3	3	—	21.83	21600	No solution
4	4	—	21.46	21600	No solution
5	5	—	21.02	21600	No solution

Table A8: Results obtained by LINDOGlobal for 2loopsNet.

n_v	n_b	UB	LB	CPU Time (s)	Status
1	1	—	—	21600	No solution
2	2	—	95.4	21600	No solution
3	3	—	93.1	21600	No solution

Table A9: Results obtained by LINDOGlobal for pescara.

n_v	n_b	UB	LB	CPU Time (s)	Status
1	1	—	—	21600	No solution
2	2	—	—	21600	No solution
3	3	—	—	21600	No solution
4	4	—	—	21600	No solution
5	5	—	—	21600	No solution

Table A10: Results obtained by couenne for 2loopsNet.

n_v	n_b	UB	LB	CPU Time (s)	Status
1	1	—	95.01	21600	No solution
2	2	—	95	21600	No solution
3	3	—	92.71	21600	No solution

Table A11: Results obtained by `couenne` for `pescara`.

n_v	n_b	UB	LB	CPU Time (s)	Status
1	1	–	24.87	21600	No solution
2	2	–	22.12	21600	No solution
3	3	–	20.93	21600	No solution
4	4	–	–	21600	No solution
5	5	–	–	21600	No solution

Table A12: Results obtained by `bonmin` for `2loopsNet`.

n_v	n_b	UB	CPU Time (s)	Status
1	1	–	21600	No solution
2	2	101.57	21600	Integer solution
3	3	–	21600	No solution

Table A13: Results obtained by `bonmin` for `pescara`.

n_v	n_b	UB	CPU Time (s)	Status
1	1	–	21600	No solution
2	2	–	21600	No solution
3	3	–	21600	No solution
4	4	–	21600	No solution
5	5	–	21600	No solution

Table A14: Results obtained by `Knitro` for `2loopsNet`.

n_v	n_b	UB	CPU Time (s)	Status
1	1	–	21600	No solution
2	2	–	21600	No solution
3	3	–	21600	No solution

Table A15: Results obtained by `Knitro` for `pescara`.

n_v	n_b	UB	CPU Time (s)	Status
1	1	–	21600	No solution
2	2	–	21600	No solution
3	3	–	21600	No solution
4	4	–	21600	No solution
5	5	–	21600	No solution

Table A16: Results obtained by `Ipopt` for `2loopsNet`.

n_v	n_b	UB	CPU Time (s)	Status
1	1	–	9.07	Conv. local infeas.
2	2	–	24.4	Conv. local infeas.
3	3	–	10.08	Conv. local infeas.

Table A17: Results obtained by Ipopt for pescara.

n_v	n_b	UB	CPU Time (s)	Status
1	1	—	2308.81	Conv. local infeas.
2	2	—	819.85	Conv. local infeas.
3	3	—	1592.12	Conv. local infeas.
4	4	—	1577.6	Conv. local infeas.
5	5	—	812.55	Conv. local infeas.

Table A18: Results obtained by AlphaECP for 21loopsNet.

n_v	n_b	UB	CPU Time (s)	Status
1	1	—	21600	No solution
2	2	100.19	21600	Integer solution
3	3	97.9	21600	Integer solution

Table A19: Results obtained by AlphaECP for pescara.

n_v	n_b	UB	CPU Time (s)	Status
1	1	—	21600	No solution
2	2	—	21600	No solution
3	3	—	21600	No solution
4	4	—	21600	No solution
5	5	—	21600	No solution

Table A20: Results obtained by RTR for 21loopsNet.

n_v	n_b	Gap (%)	UB	LB	CPU Time (s)
1	0	6.26	106.05	99.8	6.68
1	1	6.17	105.77	99.63	6.54
1	2	5.95	105.56	99.63	6.29
1	3	5.92	105.53	99.63	6.31
2	0	5.08	100.65	95.79	5.89
2	1	4.8	100.26	95.66	5.89
2	2	4.67	100.13	95.66	5.94
2	3	4.64	100.1	95.66	5.7
3	0	5.48	98.35	93.24	5.48
3	1	5.18	97.96	93.14	5.45
3	2	5.05	97.84	93.14	5.5
3	3	5.01	97.8	93.14	5.53

Table A21: Results obtained by RTR for pescara.

n_v	n_b	Gap (%)	UB	LB	CPU Time (s)
1	0	27.39	44.31	34.78	1304.52
1	1	27.42	44.09	34.6	1324.84
1	2	26.97	43.94	34.6	1310.12
1	3	26.76	43.86	34.6	1311.94
1	4	26.69	43.84	34.6	1314.38
1	5	26.66	43.83	34.6	1386.77
2	0	32.51	35.18	26.55	929.12
2	1	32.32	34.99	26.44	953.04
2	2	31.8	34.85	26.44	941.77
2	3	31.37	34.74	26.44	945.98
2	4	31.27	34.71	26.44	952.27
2	5	31.24	34.7	26.44	1057.39
3	0	29.32	28.98	22.41	588.54
3	1	29.1	28.77	22.29	607.26
3	2	28.23	28.58	22.29	598.21
3	3	28	28.53	22.29	602.77
3	4	27.89	28.5	22.29	604.91
3	5	27.86	28.5	22.29	687.47
4	0	32.59	28.03	21.14	216
4	1	32.17	27.82	21.05	236.77
4	2	31.28	27.63	21.05	230.53
4	3	31.03	27.58	21.05	232.09
4	4	30.91	27.55	21.05	230.9
4	5	30.88	27.55	21.05	328.02
5	0	35.65	27.68	20.41	210.3
5	1	35.15	27.47	20.33	233.78
5	2	34.23	27.29	20.33	223.26
5	3	33.98	27.24	20.33	223.86
5	4	33.85	27.21	20.33	224.49
5	5	33.82	27.2	20.33	309.78

Table A22: Results obtained by RTR for modena.

n_v	n_b	Gap (%)	UB	LB	CPU Time (s)
1	0	19.55	66.58	55.7	3961.52
1	1	19.35	66.43	55.66	4054.75
1	2	19.13	66.31	55.66	4197.41
1	3	18.92	66.19	55.66	5005.25
1	4	18.78	66.11	55.66	5064.04
1	5	18.76	66.1	55.66	9002.53
2	0	17.45	61.22	52.12	2382.6
2	1	17.16	61.07	52.12	2488.16
2	2	16.91	60.93	52.12	2812.11
2	3	16.66	60.81	52.12	3275.83
2	4	16.55	60.75	52.12	4287.42
2	5	16.53	60.74	52.12	10131.5
3	0	12.2	57.07	50.86	1106.79
3	1	11.81	56.87	50.86	1229.86
3	2	11.44	56.68	50.86	1223.84
3	3	11.33	56.62	50.86	1469.3
3	4	11.27	56.6	50.86	2273.58
3	5	11.26	56.59	50.86	9419.76
4	0	6.09	53.6	50.52	1065.34
4	1	5.69	53.39	50.52	1135.22
4	2	5.41	53.25	50.52	1189.47
4	3	5.26	53.18	50.52	1352.26
4	4	5.16	53.13	50.52	1794.46
4	5	5.15	53.12	50.52	4573.93
5	0	—	—	50.45	1048.34
5	1	—	—	50.45	1045.1
5	2	—	—	50.45	1052.41
5	3	—	—	50.45	1051.53
5	4	—	—	50.45	1050.66
5	5	—	—	50.45	1049.48

Acknowledgements

Filippo Pecci and Ivan Stoianov are supported by EPSRC (EP/P004229/1, Dynamically Adaptive and Resilient Water Supply Networks for a Sustainable Future). Avi Ostfeld is supported by the Israel Science Foundation (grant No. 555/18).

References

- [ARC06] L. S. Araujo, H. Ramos, and S. T. Coelho. Pressure Control for Leakage Minimization in Water Distribution Systems Management. *Water Resources Management*, 20(1):133–149, 2006.
- [Art20] Artelys. Artelys Knitro User’s Manual, 2020.
- [ASGK14] Angeliki Aisopou, Ivan Stoianov, Nigel Graham, and Bryan Karney. Analytical and experimental investigation of chlorine decay in water supply systems under unsteady hydraulic conditions. *Journal of Hydroinformatics*, 16(3):690–709, 2014.
- [BBC⁺08] Pierre Bonami, Lorenz T. Biegler, Andrew R. Conn, Gérard Cornuéjols, I. E. Grossmann, Carl D. Laird, Jon Lee, Andrea Lodi, François Margot, Nicolas Sawaya, and Andreas Wächter. An algorithmic framework for convex mixed integer nonlinear programs. *Discrete Optimization*, 5(2):186–204, 2008.
- [BDL⁺12] Cristiana Bragalli, Claudia D’Ambrosio, Jon Lee, Andrea Lodi, and Paolo Toth. On the optimal design of water distribution networks: A practical MINLP approach. *Optimization and Engineering*, 13(2):219–246, 2012.
- [BLL⁺09] Pietro Belotti, Jon Lee, Leo Liberti, François Margot, and Andreas Wächter. Branching and bounds tightening techniques for non-convex MINLP. *Optimization Methods and Software*, 24(4-5):597–634, 2009.
- [BTU⁺98] Dominic L. Boccelli, Michael E. Tryby, James G. Uber, Lewis A. Rossman, Michael L. Zierolf, and Marios M. Polycarpou. Optimal scheduling of booster disinfection in water distribution networks. *Journal of Water Resources Planning and Management*, 124(2):99–111, 1998.
- [CMM98] Joseph Czyzyk, Michael P. Mesnier, and Jorge J. Moré. The neos server. *IEEE Journal on Computational Science and Engineering*, 5(3):68 — 75, 1998.
- [DLWB15] Claudia D’Ambrosio, Andrea Lodi, Sven Wiese, and Cristiana Bragalli. Mathematical programming techniques in water network optimization. *European Journal of Operational Research*, 243(3):774–788, 2015.
- [EM12] Bradley J. Eck and Martin Mevissen. Non-Linear Optimization with Quadratic Pipe Friction. Technical Report RC25307, IBM Research Division, 2012.
- [EM15] Bradley J. Eck and Martin Mevissen. Quadratic approximations for pipe friction. *Journal of Hydroinformatics*, 17(3):462–472, 2015.

- [GEG⁺17] Ambros Gleixner, Leon Eifler, Tristan Gally, Gerald Gamrath, Patrick Gemander, Robert Lion Gottwald, Gregor Hendel, Christopher Hojny, Thorsten Koch, Matthias Miltenberger, Benjamin Müller, Marc E. Pfetsch, Christian Puchert, Daniel Rehfeldt, Franziska Schlotzner, Felipe Serrano, Yuji Shinano, Jan Merlin Viernickel, Stefan Vigerske, Dieter Weninger, Jonas T. Witt, and Jakob Witzig. The SCIP Optimization Suite 5.0. Technical Report 17-61, Zuse Institute Berlin, 2017.
- [Gur20] Gurobi Optimization. Gurobi Optimizer 9.0 Reference Manual, 2020.
- [HWF⁺02] N. B. Hallam, J. R. West, C. F. Forster, J. C. Powell, and I. Spencer. The decay of chlorine associated with the pipe wall in water distribution systems. *Water Research*, 36(14):3479–3488, 2002.
- [ICC99] M. Rashidul Islam, M. Hanif Chaudhry, and Robert M. Clark. Inverse modeling of chlorine concentration in pipe networks under dynamic condition. *Journal of Environmental Engineering*, 125(3):296–298, 1999.
- [KL10] Doosun Kang and Kevin Lansey. Real-Time optimal valve operation and booster disinfection for water quality in water distribution systems. *Journal of Water Resources Planning and Management*, 136(4):463–473, 2010.
- [Lin20] Lindo Systems, Inc., 2020.
- [NZ09] Matteo Nicolini and Luigino Zovatto. Optimal Location and Control of Pressure Reducing Valves in Water Networks. *Journal of Water Resources Planning and Management*, 135(3):178–187, 2009.
- [Ost05] Avi Ostfeld. Optimal Design and Operation of Multiquality Networks under Unsteady Conditions. *Journal of Water Resources Planning and Management*, 131(April):116–124, 2005.
- [PAS17] Filippo Pecci, Edo Abraham, and Ivan Stoianov. Quadratic Head Loss Approximations for Optimisation of Problems in Water Supply Networks. *Journal of Hydroinformatics*, 19(4):493–506, 7 2017.
- [PAS19] Filippo Pecci, Edo Abraham, and Ivan Stoianov. Global optimality bounds for the placement of control valves in water supply networks. *Optimization and Engineering*, 20:457–495, 2019.
- [PU04] Marco Propato and James G. Uber. Booster System Design Using Mixed-Integer Quadratic Programming. *Journal of Water Resources Planning and Management*, 130(4):348–352, 2004.
- [QWM⁺20] Richard S. Quilliam, Manfred Weidmann, Vanessa Moresco, Heather Purshouse, Zoe O’Hara, and David M. Oliver. COVID-19: The environmental implications of shedding SARS-CoV-2 in human faeces. *Environment international*, 140(April):105790, 2020.
- [RB96] Lewis A. Rossman and Paul F. Boulos. Numerical methods for modeling water quality in distribution systems: A comparison. *Journal of Water Resources Planning and Management*, 122(2):137–146, 1996.

- [SA99] Hanif D. Sherali and Warren P. Adams. *A Reformulation-Linearization Technique for Solving Discrete and Continuous Nonconvex Problems*. Springer, Boston, MA, 1999.
- [SLA20] Takuya Sakomoto, Mahmood Lutaaya, and Edo Abraham. Managing water quality in intermittent supply systems: The Case of Mukono Town, Uganda. *Water (Switzerland)*, 12(3), 2020.
- [TS02] Mohit Tawarmalani and Nikolaos V. Sahinidis. *Convexification and Global Optimization in Continuous and Mixed-Integer Nonlinear Programming*. Springer US, 1 edition, 2002.
- [WAPS15] Robert Wright, Edo Abraham, Panos Parpas, and Ivan Stoianov. Control of water distribution networks with dynamic DMA topology using strictly feasible sequential convex programming. *Water Resources Research*, 51(12):9925–9941, 2015.
- [WB06] Andreas Waechter and Lorenz T. Biegler. On the Implementation of a Primal-Dual Interior Point Filter Line Search Algorithm for Large-Scale Nonlinear Programming. *Mathematical Programming*, 106(1):25–57, 2006.
- [WP02] T. Westerlund and P. Pörn. Solving pseudo-convex mixed integer optimization problems by cutting plane techniques. *Optimization and Engineering*, 3(3):253 — 280, 2002.
- [WPS20] Alexander Waldron, Filippo Pecci, and Ivan Stoianov. Regularisation of an inverse problem for parameter estimation in water distribution networks. *Journal of Water Resources Planning and Management*, 146(9):04020076, 2020.